

Street Network created by Proximity Graphs: Its Topological Structure and Travel Efficiency

Toshihiro Osaragi
Tokyo Institute of
Technology
2-12-1 O-okayama,
Meguro-ku, Tokyo, Japan
osaragi@mei.titech.ac.jp

Yuko Hiraga
Tokyo Institute of
Technology
2-12-1 O-okayama,
Meguro-ku, Tokyo, Japan
hiraga@os.mei.titech.ac.jp

Abstract

There exists a large body of basic research on street networks using proximity graphs from various viewpoints. In the present study, we employ proximity graphs based on β -skeletons which change in response to variations in parameter values of β , and attempt to analyze street networks from the viewpoint of the topological structure and the travel efficiency at the same time. Some new findings on their relationships are demonstrated by numerical case studies on street networks created by proximity graphs.

keywords: street network; proximity graph; β -skeleton; topological structure; travel efficiency; spanning ratio

1 Introduction

Proximity graphs, also called neighborhood graphs, are simply graphs in which two vertices are connected by an edge if and only if the vertices satisfy particular geometric requirements. “Proximity” here means spatial distance, and many of them can be formulated with respect to many metrics, but the Euclidean metric is used most frequently [4]. These graphs are utilized in multiple applications. For instance, in computer science, properties, bounds on the size, algorithms, and variants of the proximity graphs were discussed, and numerous applications including computational morphology, spatial analysis, pattern classification, and data bases for computer vision were described [7].

In spatial analysis, Tanimura and Furuyama [16] and Watanabe [18] created familiar proximity graphs (Delaunay triangulations, Gabriel graphs, relative neighbourhood graphs, and minimum spanning trees) using the locations of intersection points in actual street networks, and discovered that such networks resemble proximity graphs.

One other area of interest where proximity graphs find application is in the field of transportation, where a graph representation of infrastructure can be used to assess efficiency of travel, configuration, properties of street networks. For instance, Koshizuka and Kobayashi [12] analyzed street networks by looking at the efficiency of travel, specifically, the ratio between shortest path length and Euclidean distance. This ratio is called “*spanning ratio*”, which has been studied theoretically and numerically using proximity graphs. Eppstein [6] discussed the dilation of various proximity graphs, defined as the maximum ratio between shortest path length and Euclidean distance. Bose [3] and Wang et al. [17] discussed theoretically the spanning ratio of a proximity graph defined on n points in the Euclidean plane, and obtained the upper-bounds and lower-bounds of the spanning ratio. Watanabe [19] evaluated the configuration and the travel efficiency on proximity graphs.

Thus, proximity graphs have been investigated from two different perspectives. From a morphological perspective the authors mainly focused on topological structure of street networks created by proximity graphs, that is, the ways in which intersections were connected [1, 13, 20]. A different approach that is relevant in transportation is the efficiency of travel, which provides an alternative perspective on networks [6, 12, 19].

In this paper, our objective is to employ the concept of β -skeleton which changes in response to variations in single parameter value of β , in order to investigate street networks from the above two different perspective: the topological structure and the travel efficiency at the same time. The original contribution of this paper is to clarify their relationships which vary according to local geographic characteristics.

2 Topological Structure of Proximity Graphs

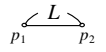
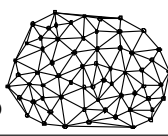
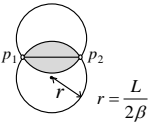
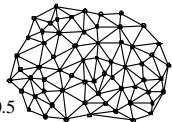
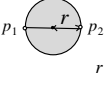
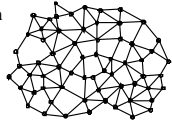
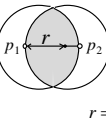

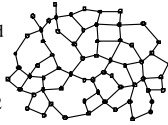
2.1 Concept of β -skeleton

Given a spatial distribution of points p_i ($i = 1, 2, \dots, n$) in two-dimensional space, let us consider various ways of creating proximity graphs that connect the points to each other. As shown in Figure 1, let us assume that two circular arcs pass through the arbitrary points p_1 and p_2 . The size of the closed region E enclosed by the arcs (the crosshatched portions in Figure 1) varies with the parameter β (≥ 0), such that the area of E increases as β increases. Then, if some third point is included within E , then the segment with endpoints p_1 and p_2 is not an edge in the graph, whereas if no such third point is included, the graph contains this segment as an edge.

A proximity graph created according to this rule is called the β -skeleton and its effective calculation methods were proposed [2, 4, 5, 11, 17]. It is well established that the case $\beta = 0$ corresponds to the complete graph (CG), $\beta = 1$

corresponds to the Gabriel graph (GG), and $\beta = 2$ corresponds to the relative neighbourhood graph (RNG).

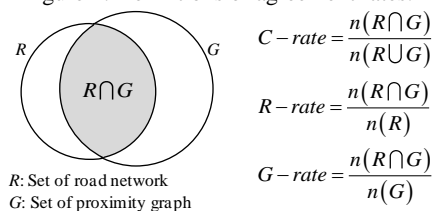
Figure 1: Definition of β -skeleton.

Range of value of β	Definition of β -skeleton	Example of Neighborhood graph
$\beta = 0$		Delaunay triangulation $\beta = 0$ 
$0 < \beta < 1$		$\beta = 0.5$ 
$\beta = 1$		Gabriel graph $\beta = 1$ 
$1 < \beta$		$\beta = 1.5$ 
		Relative neighborhood graph $\beta = 2$ 

2.2 Definition of agreement rate

Let us define an “agreement rate” as an index expressing how closely the morphology or topology of a proximity graph resembles that of an actual street network (that is, the degree of morphological or topological structure [8, 9]). First, the set of edges making up the street network is denoted by R , and the set of edges making up the proximity graph is denoted by G . The number of elements in the set of edges (number of edges) is written as the function $n(\cdot)$. Then, we define the agreement rate (C -rate) as the number of elements in $R \cap G$ divided by the number of elements in $R \cup G$, that is, $n(R \cap G)/n(R \cup G)$. Also, we distinguish between what we call the “ R -rate”, an alternative agreement rate based on the actual street network R , $n(R \cap G)/n(R)$, and the “ G -rate”, an alternative agreement rate based on the proximity graph G , $n(R \cap G)/n(G)$.

Figure 2: Definitions of agreement rates.



2.3 Maximum agreement rate and value of β

A part of the greater Tokyo metropolitan region was chosen as the area for analysis (Figure 3). The analytical region was subdivided into eight subregions according to map borders (as indicated by the numerals in the figure), and each subregion was analyzed in order to consider local characteristics. The highways in each subregion were extracted as the actual street network R (Figure 4). Because the objective is to analyze similarity of topological structure, all the streets between the intersection points of the street network were replaced with straight lines.

Figure 3: Study area.

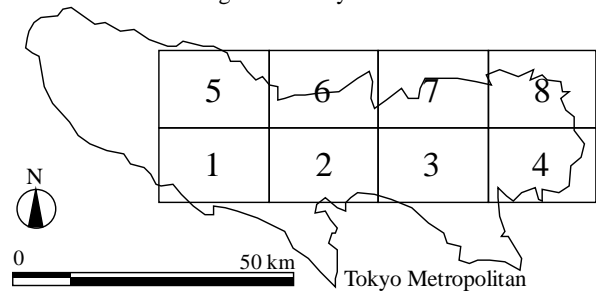


Figure 4: Street networks to be analyzed as R .

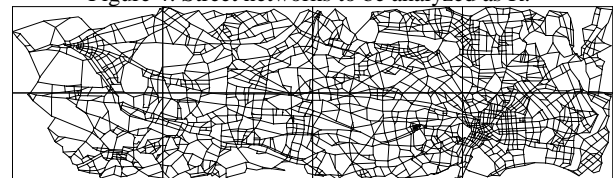


Figure 5 is a set of proximity graphs G in which β is varied from 1.0 to 2.0 in steps of 0.5 using the actual intersection points in Figure 4. As seen, the number of edges decreases gradually as the value of β increases.

In Figure 6 (a), the edges in the actual street network R are shown with the portion common with the proximity graph G ($\beta = 1.5$) ($R \cap G$) indicated by thick lines. In Figure 6 (b), the proximity graph G ($\beta = 1.5$) is shown, again with the common portion with the actual street networks ($R \cap G$) indicated by thick lines.

Proximity graphs G were created for various values of β , using Subregion 4 as an example, and the resulting C -rate, R -rate, and G -rate with respect to the actual street network were calculated (shown in Figure 7). The value of β yielding the maximum agreement rate is labeled β_1 . There is a trade-off between maximizing the G -rate and maximizing the R -rate, but the agreement rate (C -rate) is a comprehensive index providing a balance between the two.

The agreement rate (C -rate) for each of the eight subregions in the study area were calculated after creating proximity graphs G for various values of β . Table 1 shows the maximum agreement rate and the corresponding β_1 . As shown, the values of β_1 for the subregions lie between 1.1 and 1.5.

Figure 5: Proximity graphs based on β -skeletons for different values of β .

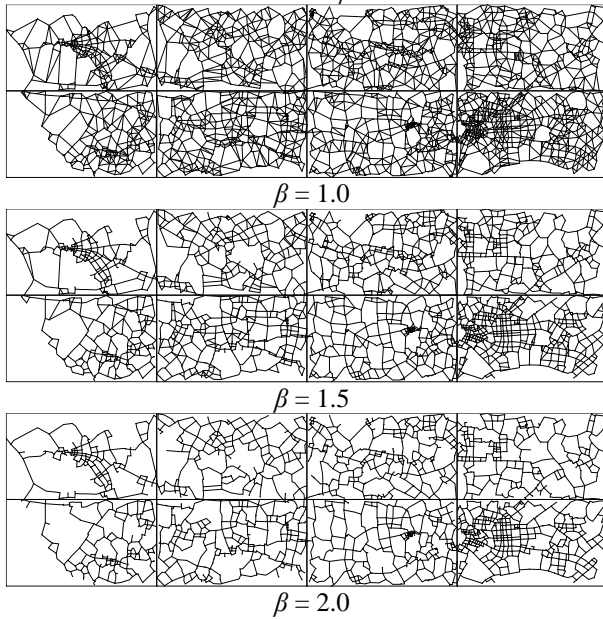


Figure 6: Common (thick lines) and disjoint (thin lines) edges of the street network R (a) and proximity graph G (b), where $\beta = 1.5$ for Subregion 4.

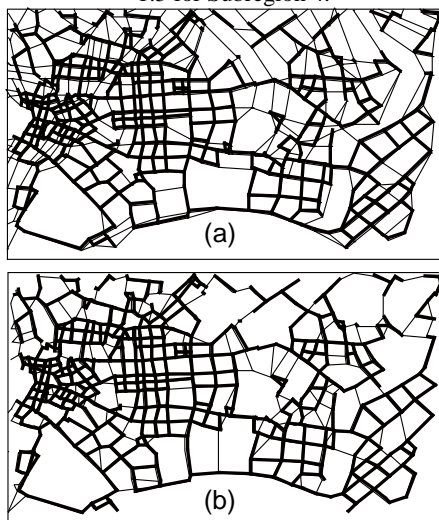


Figure 7: Agreement rate as function of β for Subregion 4.

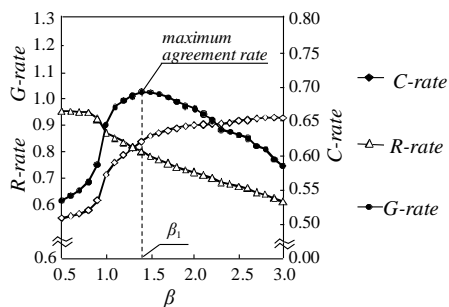


Table 1: Maximum agreement rate and the corresponding value of β_1 .

Subregion	Maximum agreement rate	β_1
1	0.610	1.40
2	0.643	1.45
3	0.639	1.15
4	0.693	1.40
5	0.623	1.20
6	0.614	1.20
7	0.637	1.30
8	0.656	1.25

2.4 Relation between maximum agreement rate and density of intersection points

Figure 8 demonstrates how the maximum agreement rate varied with the density of intersection points (the number of intersections per square kilometer). The highest β_1 in the Tokyo region is for Subregion 4, where the density of intersection points is greatest; β_1 is lowest in Subregions 1, 5, and 6, which have the low densities of intersection points.

Let us consider why the agreement rate is low for these areas, such as mountainous areas, where the density of intersection points is low. As shown in Figure 9, builders of actual street networks tend to skirt mountainous areas, so spatially neighboring points p_1 and p_2 , as well as points p_3 and p_4 , are not directly connected to each other. However, in proximity graph G , only the spatial relationships are considered, and so the agreement rate was lowered by the addition of edges between such points.

Figure 8: Maximum agreement rate versus density of intersection points (numerals indicate subregion)

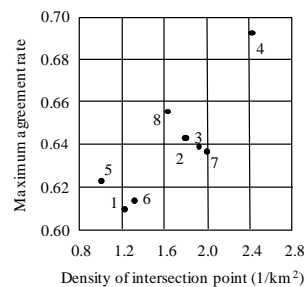
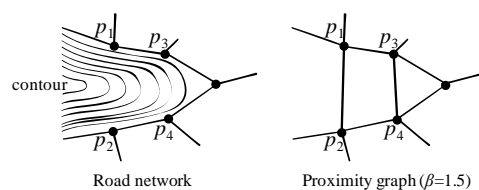


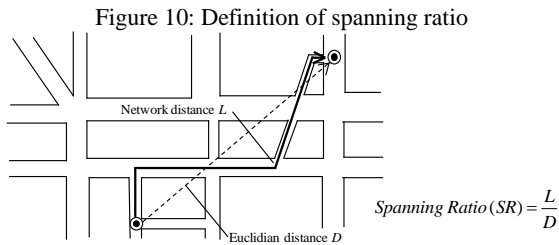
Figure 9: Explanation of low agreement rates for mountainous areas



3 Travel Efficiency of Proximity Graphs

3.1 Concept of spanning ratio

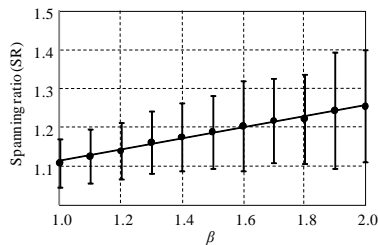
The spanning ratio (*SR*) has been suggested as an index expressing the travel efficiency through a network [3, 17]. *SR* is defined as the value of the distance *L* between two points on the network paths divided by the Euclidian distance *D* between the points (Figure 10). In other words, the greater the values *SR*, the lower the travel efficiency in the network.



3.2 Spanning ratio of proximity graphs

The intersection points in the street networks *R* in the previous section were used to create proximity graphs for various values of β ($1.0 \leq \beta \leq 2.0$). Next, two intersections at a time were extracted at random and the value of *SR* was calculated for that pair. The mean *m* and standard deviation σ were calculated for the *SR* of 1,000 point pairs for each graph. The results showed that *m* is an increasing linear function of β ($m = a\beta + b$; *a* and *b* are unknown parameters). The increase in *m* is due to proximity graphs with higher values of β having lower numbers of edges, decreasing the efficiency of spatial movement in the graphs (Figure 11).

Figure 11: Mean and standard deviation (indicated by error bars) of spanning ratio of proximity graphs *G* for Subregion 4.



Also, the results showed that the value of σ grows with the value of β . The growth of σ indicates that there is high variation in the travel efficiency between point pairs, that is, that there is a large difference between the Euclidian distance and the network distance between point pairs. Therefore, when we conduct analysis of spatial movement in regions with low street densities, it is preferable to use network distance rather than Euclidian distance.

The mean *m* of *SR* for 1,000 point pairs was calculated for the actual street network of each subregion. The values of β (β_2) were then inversely estimated using *m* by the equations ($\beta_2 = (m - b)/a$). Specifically, the values of β for the proximity graph indicating the mean values of *SR* equivalent to that of the actual street network were calculated. These values are

shown in Table 2 along with the corresponding values for parameters of regression equations. As shown, in all the subregions analyzed here, β_2 remains within the range 1.1 to 1.5, the same as β_1 .

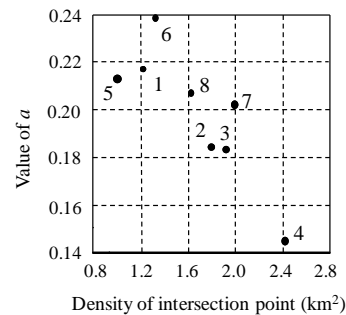
Table 2: Value of β_2 for the proximity graph whose travel efficiency is equivalent to that of actual street network.

Subregion	<i>m</i>	<i>a</i>	<i>b</i>	<i>R</i> ²	β_2
1	1.224	0.217	0.913	0.993	1.440
2	1.196	0.184	0.934	0.993	1.432
3	1.155	0.184	0.946	0.981	1.146
4	1.166	0.145	0.968	0.993	1.363
5	1.184	0.213	0.906	0.998	1.310
6	1.194	0.238	0.874	0.994	1.350
7	1.178	0.202	0.914	0.989	1.310
8	1.210	0.207	0.918	0.995	1.374

3.3 Relation between spanning ratio and density of intersection points

Figure 12 shows how the slopes *a* in Table 2 varied by the density of intersection points. As shown, the lower the density, the greater the slope. Since slope *a* indicates the rate of increase in *SR* with respect to an increase in β (from the regression equation $SR = a\beta + b$), the lower the density of streets in a region, the greater the influence of β on travel efficiency (*SR*) in the corresponding proximity graphs. Thus, the travel efficiency in an area with a low density of intersection points will be more strongly influenced by street closures, for example due to earthquakes, than higher density areas.

Figure 12: Slope *a* versus density of intersection points (numerals indicate subregion)

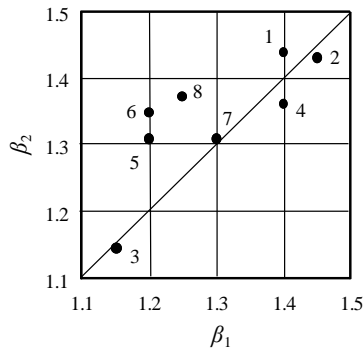


3.4 Relation between β_1 and β_2

Figure 13 shows relationships between the β_1 (value of β for proximity of topological structure) and the β_2 (value of β for proximity of travel efficiency). The values of β_1 and β_2 are roughly similar in subregions 1, 2, 3, 4, and 7, mainly the downtown Tokyo area, where the density of streets is high. On the other hand, in subregions 5, 6, and 8, suburban areas with low densities of streets or areas with mountains or wide rivers, $\beta_1 < \beta_2$ holds. In these areas, there is a risk that using proximity graphs, which have been created on the basis of proximity of topological structure, will provide erroneous predictions of travel efficiency. Specifically, the travel

efficiency in the actual street network is likely to be lower than that in the proximity graph created on the basis of topological proximity in these areas.

Figure 13: β_1 versus β_2 (numerals are subregion numbers).



4 Summary and Conclusions

We carried out an analysis of a street network created by proximity graphs based on β -skeletons from each of two viewpoints, topological structure and travel efficiency. The following findings were identified:

(1) The value of β in a proximity graph with a maximal topological proximity to an actual street network is in the range 1.1 to 1.5 for the networks examined here.

(2) The agreement rate between a street network and a proximity graph is less in mountainous suburban areas or similar areas with low densities of streets.

(3) The value of β in a proximity graph in which travel efficiency is equivalent to an actual street network is in the range 1.1 to 1.5 for the networks examined here.

(4) The travel efficiency (Spanning Ratio: SR) between two points shows more variation in suburban areas with low densities of streets; therefore, when investigating the travel efficiency between locations, the analysis must employ the distance in the network rather than the Euclidian distance between the points.

(5) The value of β_1 when there is high topological proximity was nearly equal to the value of β_2 when there is a strong similarity between the travel efficiencies in the central part of Tokyo. However, $\beta_1 < \beta_2$ in the Tokyo suburbs, indicating that an analyst must take account of the higher travel efficiency in the proximity graph mostly strongly resembling the actual street network than that in the actual street network itself.

In this paper, we investigated the properties of proximity graphs by comparing with actual street networks. This approach can be extended for the general modeling of various numerical simulations, as well as theoretical analysis on intersections which are randomly distributed following the Poisson distribution. It would be also interesting to develop this approach for the street hierarchies from the multiple perspectives of topology and geometry [10], and for a method to automate street networks in urban area [14].

Acknowledgements

The authors would like to acknowledge the valuable comments and useful suggestions from Prof. Daisuke Watanabe (Tokyo University of Marine Science and Technology) and anonymous reviewers to improve the content and clarity of the paper.

References

- [1] M. Barthélemy and A. Flammini. Modeling urban street patterns, *PHYSICAL REVIEW LETTERS*, 100(13), 138702-1-4, 2008.
- [2] M. Bhardwaj, S. Misra and G. Xue. Distributed topology control in wireless ad hoc networks using β -skeleton, *Workshop on High Performance Switching and Routing (HPSR 2005)*, Hong Kong, China, 2005.
- [3] P. Bose, L. Devroye, W. Evans and D. Kirkpatrick. On the spanning rate of Gabriel graphs and β -skeletons, *Lecture Notes in Computer Science*, 2286, 479-493, 2002.
- [4] P. Bose, J. Cardinal, S. Collette, E. D. Demaine, B. Palop, P. Taslakian and N. Zeh. Relaxed Gabriel graphs, *Proc. 15th Canadian Conference on Computational Geometry (CCCG 2009, Vancouver)*, 169-172, 2009.
- [5] J. Cardinal, S. Collette and S. Langerman. Empty region graphs, *Computational Geometry*, 42(3), 183-195, 2009.
- [6] D. Eppstein. Beta-skeletons have unbounded dilation, *Computational Geometry Theory & Applications*, 23(1), 43-52, 2002.
- [7] W. J. Jaromczyk and G. T. Toussaint. Relative neighbourhood graphs and their relatives, *Proc. IEEE*, 80, 1502-1517, 1992.
- [8] B. Jiang and C. Claramunt. Topological analysis of urban street networks, *Environment and Planning B: Planning and Design*, 31, 151-162, 2004a.
- [9] B. Jiang and C. Claramunt. A structural approach to the model generalization of an urban street network, *GeoInformatica*, 8(2), 157-171, 2004b.
- [10] B. Jiang. Street hierarchies: a minority of streets account for a majority of traffic flow, *International Journal of Geographical Information Science*, 23(8), 1033-1048, 2009.
- [11] F. Hurtado, G. Liotta and H. Meijer. Optimal and suboptimal robust algorithms for proximity graphs, *Computational Geometry Theory & Applications*, 25(1-2), 35-49, 2003.
- [12] T. Koshizuka and J. Kobayashi. On the relation between street distance and Euclidean distance, *City planning review*, 18, 43-48, 1983.
- [13] S. Porta, P. Crucitti and V. Latora. The network analysis of urban streets: A dual approach, *Physica A: Statistical Mechanics and its Applications*, 369(2), 853-866, 2006.
- [14] J. Radke and A. Flodmark. The use of spatial decompositions for constructing street centerlines, *Geographic Information Sciences*, 5(1), 15-23, 1999.
- [15] C. Ratti. Urban texture and space syntax: some inconsistencies, *Environment and Planning B: Planning and Design*, 31, 151-162, 2004.

- [16] T. Tanimura and M. Furuyama. A study on the rational network morphology embedded in English historic town, *Journal of architecture, planning and environmental engineering, Transactions of AIJ*, 563:179-186, 2002.
- [17] W. Wang, X. Y. Li, K. Moaveninejad, Y. Wang and W. Z. Song. The spanning ratio of β -skeletons, *Proc. 15th Canadian Conference on Computational Geometry (CCCG 2003, Halifax)*, 35–38, 2003.
- [18] D. Watanabe. A study on analysing the street network pattern using proximity graphs, *Journal of the City Planning Institute of Japan*, 40, 133-138, 2005.
- [19] D. Watanabe. Evaluating the configuration and the travel efficiency on proximity graphs as transportation networks, *FORMA*, 23(2), 81-87, 2008.
- [20] D. Watanabe. A study on analyzing the grid road network patterns using relative neighborhood graph, *The Ninth International Symposium on Operations Research and Its Applications (ISORA'10)*, 112–119, 2010.